Conference on Modelling Fluid Flow
(CMFF'06)
The 13th International Conference on Fluid Flow Technologies
Budapest, Hungary, September 6-9, 2006

THE EFFECT OF CORNER RADIUS ON THE ENERGY LOSS IN 90° T-JUNCTION TURBULENT FLOWS

György PAÁL[1], Fernando PINHO[2], Rodrigo MAIA[3]

[1] Corresponding author, Department of Hydrodynamic Systems, Budapest University of Technology and Economics, P.O. Box 91, 1521 Budapest, HUNGARY, Tel.: +36 1 463 2991, Fax: +36 1 463 3091, E-mail: paal@vizgep.bme.hu
[2] Transport Phenomena Research Center, Faculty of Engineering, University of Porto and University of Minho E-mail: fpinho@fe.up.pt
[3] Department of Civil Engineering, Faculty of Engineering, University of Porto, E-mail: rmaia@fe.up.pt

ABSTRACT

An extensive numerical parametric investigation of the turbulent flow in 90° T-junctions with sharp and rounded corners is under way aimed at quantifying the energy losses and the size and strength of the recirculating region in the branch pipe. The parameter that is being investigated is the radius of curvature of the corner of the junction and so far simulations have been carried out for an inlet pipe Reynolds numbers of 32,000, to be later extended to the range between 5,000 and 40,000, for flow rate ratios of 0%, 20%, 40%, 50%, 60%, 80% and 100% (ratio between the flow rates in the branch and inlet pipes).

The previous work of Paál et al. [8] on this flow for a sharp corner was aimed at validation by comparing the results of simulations done with various turbulence models with the detailed experimental data of Maia et al. (1998).

Following [8], it was decided to perform the present calculations using a modified version of Menter's [9] model, the shear-stress transport (SST) model, which performed equally well as or even better than the full Reynolds stress model at a considerably lower cost. All the calculations were carried out with the commercial code ANSYS CFX 10.0.

The results show that increasing the radius of curvature of the corner reduces the total energy loss especially because of the reduction in the branch flow loss related to flow separation.

Keywords: T-junction, turbulent flow simulation, rounded edge

NOMENCLATURE

a	[-]	turbulence model parameter
f	[-]	pipe loss coefficient
k	[m^2/s^2]	turbulent kinetic energy
p	[Pa]	pressure
Δp	[Pa]	pressure difference
t	[s]	time
u_i	[m/s]	velocity (fluct. ith comp.)
x	[m]	length coordinate
y	[m]	coordinate normal to the wall
A_i	[-]	turbulence model parameters
C	[-]	turbulence model parameters
F_i	[-]	blending functions
K_{ij}	[-]	loss coefficient due to tee
U	[m/s]	velocity (mean x-component)
V	[m/s]	velocity (mean y-component)
$<U>$	[m/s]	bulk velocity
α_i	[-]	turbulence model parameters
β_i	[-]	turbulence model parameters
δ_{ij}	[-]	Kronecker symbol
φ_i	[-]	turbulence parameters (SST)
μ	[kg/ms]	dynamic viscosity
ν	[m^2/s]	kinematic viscosity
ρ	[kg/m^3]	density
σ	[-]	turbulence model parameters
ω	[$1/s$]	turbulence frequency

Subscripts and Superscript

i, j	ith, jth coordinate, pipe identifier
k, μ, ⌉	turbulence parameter indicator
T	turbulent

1. INTRODUCTION

In pipe networks flow divergence is a major source of energy loss especially when in combination with sudden changes in flow direction leading to severe flow separations. The proper design of pipe networks requires accurate predictions of these complex flows, which is still far from being a trivial matter. In this work, we predict the loss coefficient of Newtonian fluids in 90° T-

junctions with sharp and rounded corners as a function of the flow rate ratio in the two outgoing branches, after a grid convergence study to select the adequate grid characteristics.

Early experimental work on the diverging T-junction flow took place in Munich with Vogel [1, 2] and was continued by Gardel [3]. Among other contributions to the field, reviewed in detail by Maia [4], the most well-known is the comprehensive work of Miller [5] on the resistance coefficients for various pipe accessories. Numerical predictions of this complex flow have been less common: Sierra-Espinoza et al. [6, 7] used various turbulence models and concluded that the standard and renormalization group (RNG) k-ε models could not predict the flow satisfactorily. Their predictions with the Reynolds stress model (RSM) also over-predicted significantly the extent of the recirculation region. Paál et al. [8] compared the performance of the standard RSM and Menter's [9] shear-stress transport (SST) k-ω model, and showed the superiority of the latter in spite of the fact that it is a two-equation model. This did not come totally as a surprise since the SST model was supposed to combine the advantages of the k-ε and the k-ω models, performing better in separated flows under adverse pressure gradients because of the inclusion of transport effects into the formulation of the eddy-viscosity. For details of the used models the numerical approach and the comparison see [8].

The present work is the natural continuation of Paál et al [8]: using the SST k-ω model we performed extensive calculations of the flow in the 90° T-junction to investigate the effect of rounding off the sharp edge of the corner of the junction for flow rate ratios of 0%, 20%, 40%, 50%, 60%, 80% and 100% (ratio between the flow rates in the branch and inlet pipes) at inlet pipe Reynolds number 32,000. The influence of a block-structured mesh as opposed to an unstructured mesh is also discussed. The commercial code used in this work was ANSYS CFX 10.0.

The paper is organized as follows: the governing equations and turbulence model used are briefly presented first, followed by a grid convergence study and validation by comparison with the experimental data of Costa et al. [10]. Then, the results of the parametric investigation are presented and discussed prior to the closure of the paper.

2. GOVERNING EQUATIONS

The equations to be solved for this incompressible flow are the conservation of mass Eq. (1) and momentum Eq. (2)

$$\frac{\partial U_i}{\partial x_i} = 0 \tag{1}$$

$$\frac{\partial \rho U_i}{\partial t} + \frac{\partial \rho U_j U_i}{\partial x_j} = -\frac{\partial \overline{p}}{\partial x_i} + \frac{\partial}{\partial x_j}\left[\mu\left(\frac{\partial U_i}{\partial x_j} + \frac{\partial U_j}{\partial x_i}\right) - \rho\overline{u_i u_j}\right] \tag{2}$$

where a capital letter or an overbar designate time-averaged quantities and a small letter refers to fluctuating quantities. The Reynolds stress tensor must be given by an appropriate equation or model to ensure closure of the set of equations. Here, on the basis of Paál et al. (2003) and also on the basis of further numerical experiments with the standard k-ε model only one turbulence model was used: the shear-stress transport (SST) k-ω model developed by Menter [10]. This model was found to provide the best results at a relatively modest computational cost.

In this model, the Reynolds stress is calculated by

$$-\overline{u_i u_j} = \nu_T\left(\frac{\partial U_i}{\partial x_j} + \frac{\partial U_j}{\partial x_i}\right) - \frac{2}{3}k\delta_{ij} \tag{3}$$

where the turbulent viscosity is related to single velocity and length scales of the turbulent flow, but is limited to avoid overprediction of recirculating regions. It is given by

$$\nu_T = \frac{ak}{\max\left[a\omega, SF_2\right]} \tag{4}$$

The transport equations of k and ω are

$$\frac{\partial \rho k}{\partial t} + \frac{\partial \rho U_j k}{\partial x_j} = -\rho\overline{u_i u_j}\frac{\partial U_i}{\partial x_j} + \frac{\partial}{\partial x_j}\left[\left(\mu + \frac{\rho \nu_T}{\sigma_{k3}}\right)\frac{\partial k}{\partial x_j}\right] - C_\mu \rho k \omega \tag{5}$$

$$\frac{\partial \rho \omega}{\partial t} + \frac{\partial \rho U_j \omega}{\partial x_j} = -\rho\alpha_3\frac{\omega}{k}\overline{u_i u_j}\frac{\partial U_i}{\partial x_j} - \beta_3\rho\omega^2 + \frac{\partial}{\partial x_j}\left[\left(\mu + \frac{\rho \nu_T}{\sigma_{\omega 3}}\right)\frac{\partial \omega}{\partial x_j}\right] + \frac{(1-F_1)2\rho\sigma_{\omega 2}}{\omega}\frac{\partial k}{\partial x_j}\frac{\partial \omega}{\partial x_j} \tag{6}$$

and the blending functions appearing in Eqs. (4) - (6) are

$$F_1 = \tanh(A_1^4) \text{ and } F_2 = \tanh(A_2^2) \tag{7}$$

with

$$A_1 = \min\left[\max\left(\frac{\sqrt{k}}{C_\mu \omega y}, \frac{500\nu}{y^2\omega}\right), \frac{4\rho k \sigma_{\omega 2}}{y^2 C_{k\omega}}\right] \quad (8)$$

$$A_2 = \max\left(\frac{2\sqrt{k}}{C_\mu \omega y}, \frac{500\nu}{y^2\omega}\right) \quad (9)$$

and

$$C_{k\omega} = \max\left(\frac{2\rho\sigma_{\omega 2}}{\omega}\frac{\partial k}{\partial x_j}\frac{\partial \omega}{\partial x_j}, 1.0\times 10^{-10}\right) \quad (10)$$

The parameters α_i, β_i, σ_{ki}, and σ_ω with i=3 result from a linear combination of the corresponding coefficients having i= 1 and 2 with the blending function F_1, as given by Eq. (11)

$$\phi_3 = F_1\phi_1 + (1 - F_1)\phi_2 \quad (11)$$

The remaining parameters are listed in Table 1.

3. FLOW PARAMETERS

3.1. Flow geometry

The central part of the T-piece with the coordinate system and the notation is presented in Figure 1. A 20 diameter long entrance pipe was attached to the inlet section and a 30 diameter long pipe was attached to each of the two outlet sections. The pipe diameter was everywhere 30 mm.

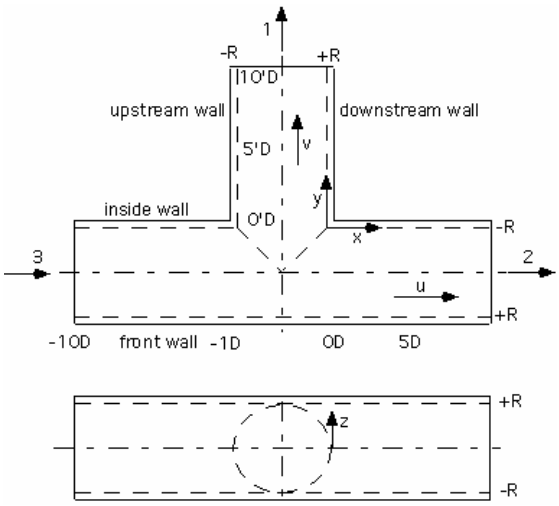

Figure 1. Schematic representation of the T-junction and the central part of the computational domain

The rounded T- piece looks very similar, except that the sharp edges are replaced with a rounded corner with a radius of 3 mm in the central plane.

Table 1. Numerical values of some parameters of the SST model

i	α_i	β_i	σ_{ki}	$\sigma_{\omega i}$
1	5/9	3/40	2	2
2	0.44	0.0828	1	0.856

3.2. Simulation parameters

The fluid used in the simulations was water with a constant density of 997 kg/m^3 and dynamic viscosity of 8.899*10^{-4} kg/ms. Incompressible flow was assumed. The inlet boundary condition was fixed at 0 Pa total pressure (as it is standard practice in incompressible fluids since only the pressure variations matter) and at the two outlets the mass flow rates were specified based on the Reynolds number and the given flow rate ratio between the two branches. Since the inlet boundary condition is located very far from the region of interest (20D = 600 mm) the actual values of the turbulent inlet boundary conditions are irrelevant because the flow is allowed to develop. At all the walls no-slip boundary conditions were assumed.

3.3. Mesh convergence studies

In the case of the sharp edge both an unstructured and a block-structured mesh have been tried with systematic mesh refinement. In both cases a similar, somewhat surprising result, to be discussed next, was obtained.

Table 2. Mesh parameters for the convergence study

Mesh	Number of elements
Coarse	61468
Fine	1004981
Fine mesh with adaptation	2287626
Fine + coarse (final mesh)	454604

First, following Paál et al. (2003), unstructured tetrahedral mesh with 5 layers of prismatic boundary layer cells was used. A systematic mesh refinement study was performed in order to determine the optimum mesh size. Due to the lack of space it is not possible here to go into all the details – they will be presented in a later publication. Altogether 3+1 meshes were used: the last one was created on the basis of the conclusions drawn from the first three. The meshes are listed in Table 2.

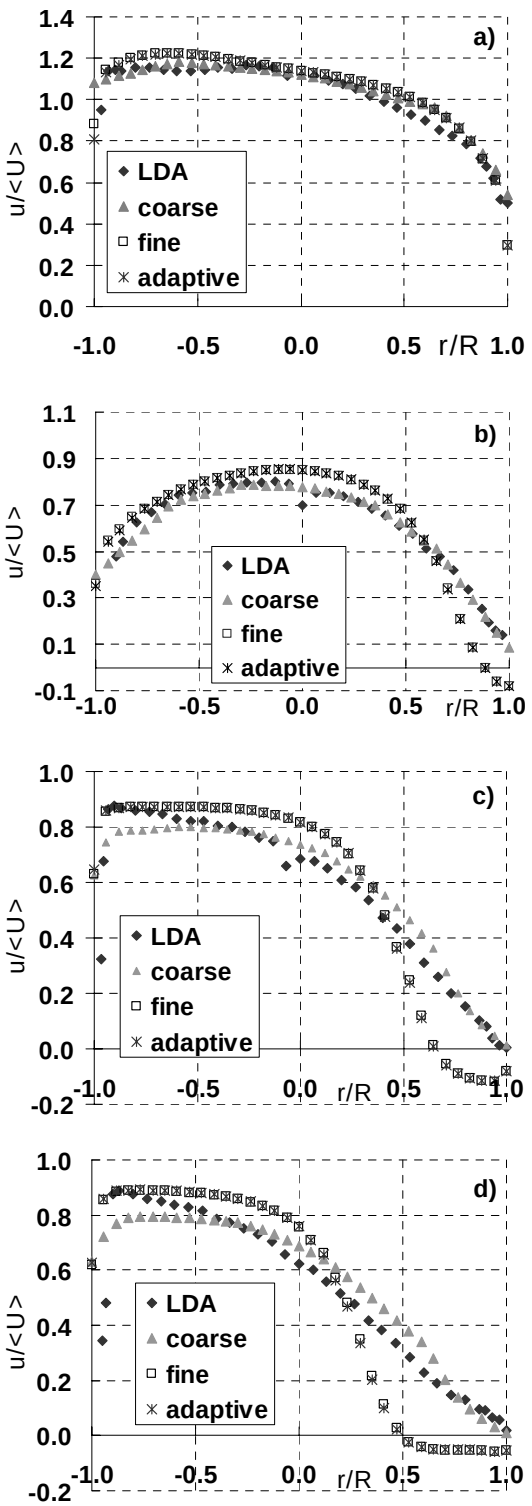

Figure 2. Longitudinal velocity profiles in the main pipe with different meshes compared with LDA data; a) -1D; b) 0D; c) 0.5D; d) 1D (sharp edge)

In Figure 2. some results can be seen with the first three meshes, compared with the LDA-data in the approach flow, inside the tee junction and in the downstream main pipe. It can be observed in the figures that in a paradoxical way the results are

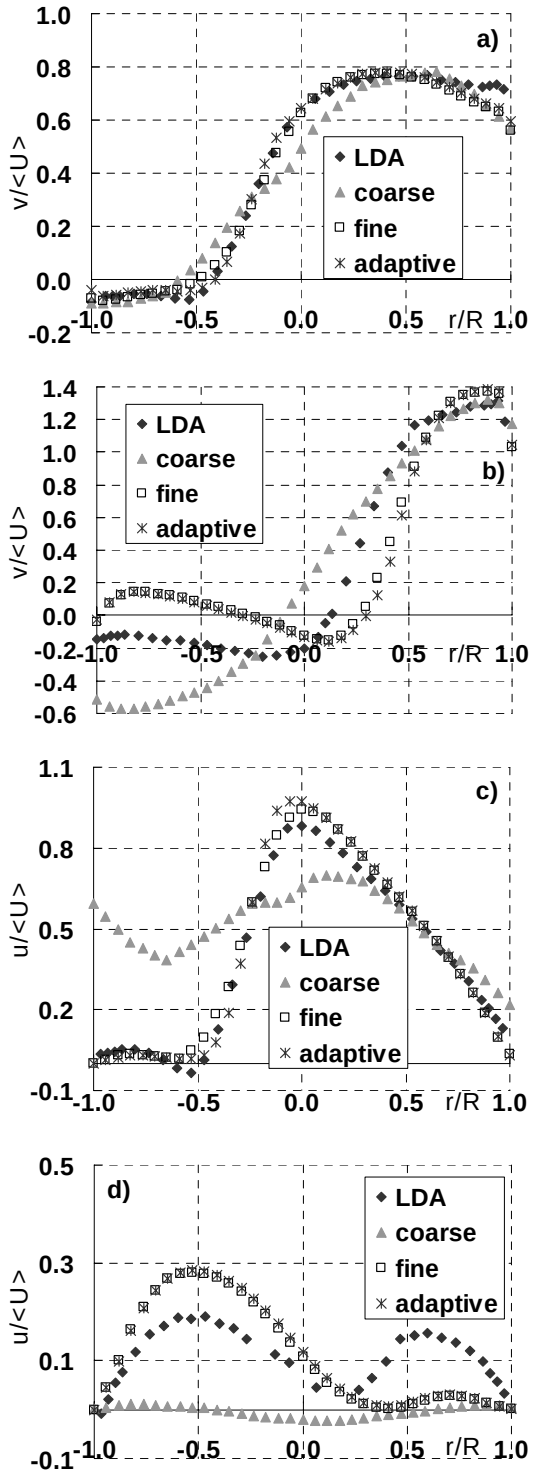

Figure 3. Velocity profiles in the branch pipe with different meshes compared with LDA data; a) longitudinal 0.1'D; b) longitudinal 1.1'D; c) transversal 0.1'D; d) transversal 1.1'D (sharp edge)

everywhere better for the coarse mesh than for the fine mesh or the fine mesh with adaptation. This

happens in the junction region and downstream in the outlet straight pipe.

One possible speculative explanation for this strange phenomenon is that the higher numerical dissipation of the coarse mesh compensates the shortcomings of the turbulence model which usually overpredicts the momentum transfer between wall and bulk flow. In the branch pipe the opposite, usual trend is observed: the fine mesh produces better results (see Figure 3.).

Although the difference is small, the fine mesh performs consistently better than the fine mesh with adaptation and much better than the coarse mesh.

Therefore the final unstructured mesh used in the simulations is a combination of the two meshes: coarse in the main pipe and fine in the branch pipe. The mesh can be seen in Figure. 4.

Due to the rather surprising result obtained with the unstructured mesh an attempt was made with a block-structured mesh with the hope that a systematic refinement of a hexagonal mesh would lead to a systematic improvement of the agreement with measurements. The coarsest mesh can be seen in Figure 5. Three finer meshes were prepared with the same block-structure and the result was the same as before: the results agreed better with the measurements with the coarse mesh in the main pipe and with the fine mesh in the branch pipe. The results are not presented here because of the lack of space, but reinforce the idea put forward above of turbulence model deficiencies being compensated by the excessive numerical diffusion with the coarse mesh.

Due to the above findings it was decided that for the further calculations the unstructured mesh is used because of its greater flexibility since the hexagonal mesh did not bring any tangible advantages.

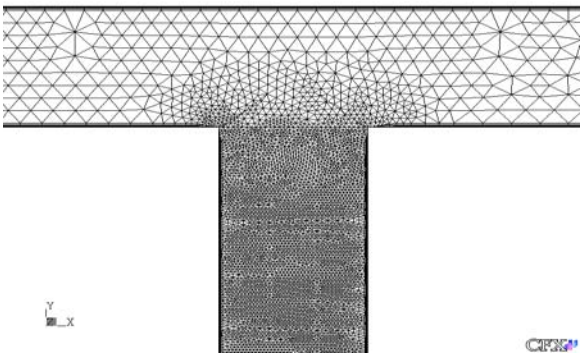

Figure 4. The final unstructured mesh used in the simulations

4. RESULTS AND DISCUSSION

The results are presented in the following way: first some mean velocity profiles of both the sharp-cornered and the rounded-cornered geometry are shown to indicate the well predicted and problematic regions. Then the pressure loss coefficients of both geometries as a function of the flow rate ratio are presented and discussed. The pressure loss coefficients of both branches are defined so that the "excess" pressure loss over the pressure loss of the straight pipe is considered. This is expressed in equations (12) and (13) where i = 1 and 2 stand for the branch and straight outlet pipes, respectively. The velocities in the brackets mean spatially averaged velocities over the cross-section.

$$K_{3i} = \frac{\Delta p_{3i}}{\frac{1}{2}\rho\langle U_3\rangle^2} \tag{12}$$

$$p_3 + \frac{1}{2}\rho\langle U_3\rangle^2 = p_i + \frac{1}{2}\rho\langle U_i\rangle^2 + \\ + f_3\frac{L_3}{D_3}\rho\langle U_3\rangle^2 + f_i\frac{L_i}{D_i}\rho\langle U_i\rangle^2 + \Delta p_{3i} \tag{13}$$

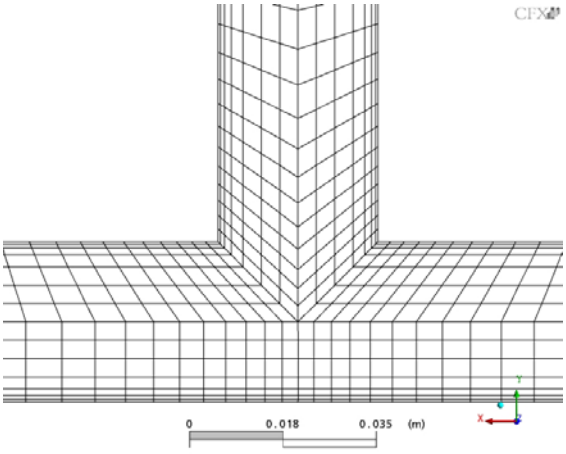

Figure 5. Block-structured mesh in the symmetry plane of the T-piece

4.1. Velocity profiles

Similarly to [8] first comparisons of LDA measurements with simulation results are presented in individual cross sections, everywhere in the symmetry plane. Due to the lack of space only a few typical profiles for the rounded edge are presented; there are also some typical figures for the sharp edge in Figures 2. and 3. Also only longitudinal mean velocity profiles are presented here, i. e. u for the main pipe and v for the branch pipe. Both the sharp edge and rounded edge geometries were measured with a flow rate ratio of 50-50% and with a Reynolds number of 32000.

Figure 6. shows the mean longitudinal velocities in the main pipe. It can be seen that in a remarkable way the agreement is very good just at the beginning of the T-junction and becomes somewhat worse further downstream. Here the velocity is constistently overpredicted near the front wall and underpredicted near the inside wall. The trends are nevertheless well captured and the

quantitative differences remain small with the exception of a few places.

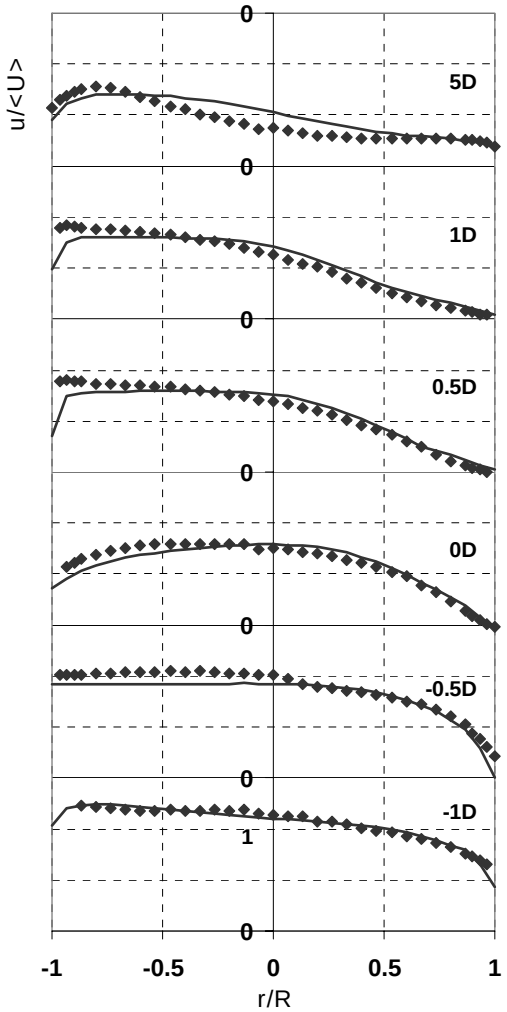

Figure 6. Comparison of the simulation and the LDA measurements for the rounded edge T-piece in the main pipe in various cross sections. Continuous line: simulation; black squares: measurements

The situation is similar in Figure 7. where the branch pipe results are presented. The quality of approximation deteriorates when getting further from the T-piece but the trends are captured everywhere well. Usually the velocity is slightly overpredicted at the downstream wall and sometimes over- sometimes underpredicted in the rest of the pipe. As a general rule we can state that the predictions in the case of the sharp-edged T-piece are slightly better than in the round T. This can be attributed partly due to the increased uncertainty of the measurements due to the complicated geometry and partly to the computational difficulties of treating a boundary layer separating from a round surface.

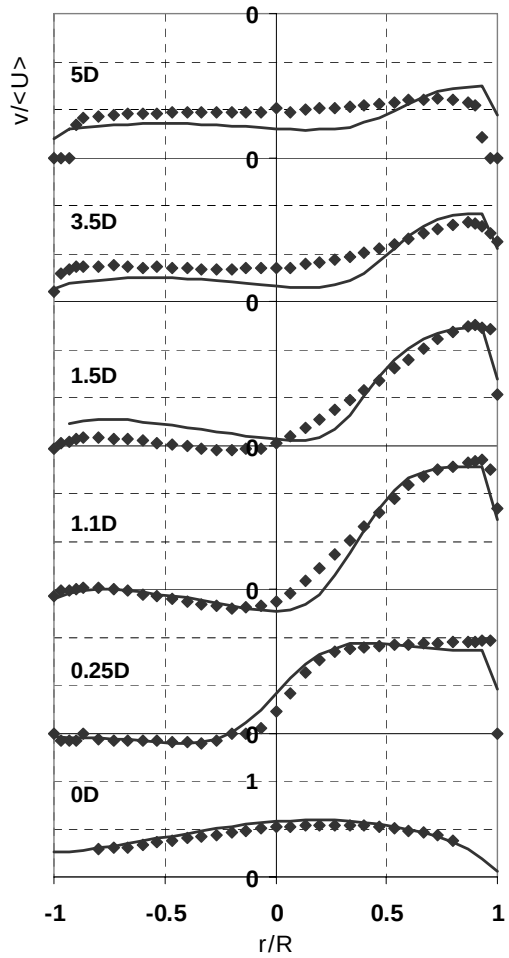

Figure 7. Comparison of the simulation and the LDA measurements for the rounded edge T-piece in the branch pipe in various cross sections. Continuous line: simulation; black squares: measurements

4.2. Loss coefficients

What is most interesting from an engineering point of view is the pressure loss caused by the presence of a T-piece. This is expressed by the nondimensional coefficients defined in Equations (12) and (13).

Although the Reynolds number differed slightly between the two cases we can assume with good reason that in this range the coefficients are almost independent of Reynolds number. Thus the two cases presented in Figs. 8 and 9 are directly comparable with each other. In the sharp-edged case the simulation reproduced the results excellently in the cases of both coefficients. There is a slight discrepancy only at high values of Q_1/Q_3.

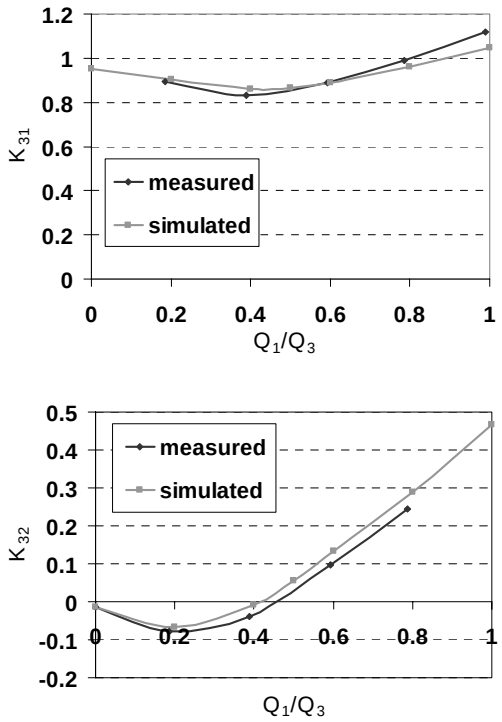

Figure 8. Loss coefficients in the sharp-edged configuration; above: K_{31}; below: K_{32}. Re = 36000.

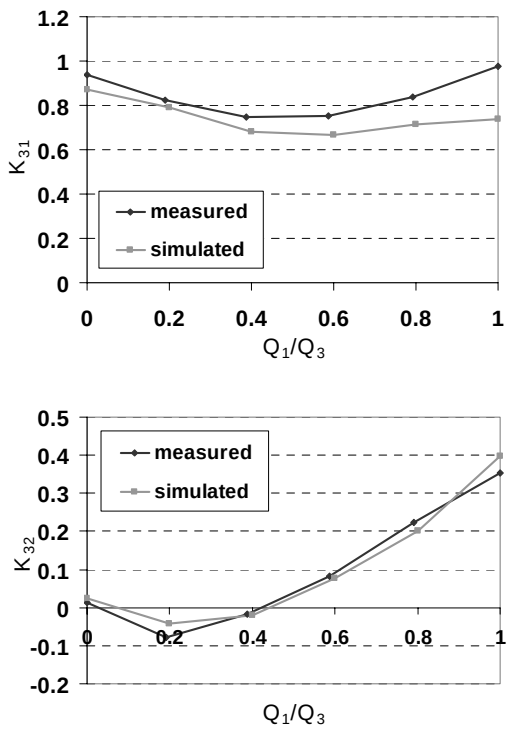

Figure 9. Loss coefficients in the round-edged configuration; above: K_{31}; below: K_{32}. *Re* = 40000

Both curves display a minimum; K_{31} between 0.4 and 0.6 K_{32} at around 0.2. The values of K_{31} are high: they lie between about 0.85 and 1.1 whereas the values of K_{32} are more moderate, between -0.08 and 0.47. However, that the values of K_{32} cover a much wider range, meaning that its dependence on the flow rate ratio is much stronger than that of K_{31}. The fact that K_{32} takes negative values might seem surprising but in reality it is not. It simply expresses the fact that under those conditions the loss caused by the T-piece in the main flow direction is slightly less than the loss would be from a fully-developed flow in a straight pipe. This is probably caused by decreases in the shear rates at the wall, and hence shear stresses, within the junction region due to the flow deviation into the branch.

If we look at Fig. 9 we can see that the agreement for the round-edge configuration, between measurement and simulation is still very good for K_{32}, but less satisfactory for K_{31}. This could be already expected from the less satisfactory agreement of the individual velocity profiles. Nevertheless the trends are again reproduced well. The places of minimum and maximum are at the same place. There is not much change between the two cases for K_{32} but there is a significant decrease in the loss coefficient for the branch pipe. This corresponds to the expectations since rounding the edge should influence mostly the loss in the branch pipe by making the point of separation less well defined.

Looking at the loss coefficients from the measurements [10] we can establish that the Reynolds number dependence in this range is really small.

4.3. Fixed point in the velocity profile?

In the sharp-edged case an interesting phenomenon was observed. Plotting the velocity profiles in the symmetry plane in one diagram for different flow rate ratios at one cross section in the branch pipe it is obvious that all the velocity profiles intersect each other more or less at the same point (Figure 10.).

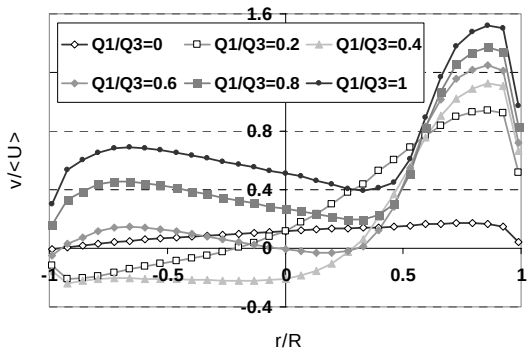

Figure 10. Velocity profiles for different flow rates intersect in one point

Repeating the same procedure for several cross sections the set of intersection points can be plotted (Figure 11.). Along this line on the symmetry plane the velocity is always the same, independently of

the flow rate ratio. On the upstream side of this line the velocity decreases, on the downstream side it increases with increasing flow rate ratio in the branch pipe. Interestingly, no similar phenomenon has been observed in the case of the round-edged T-piece, because the point of separation changes with flow rate ratio.

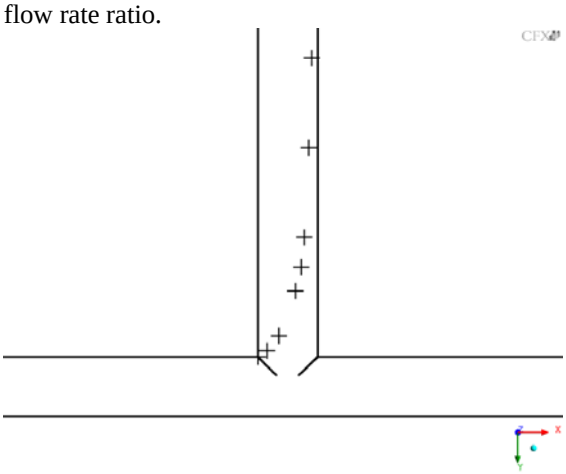

Figure 11. Set of "fixed points" in the symmetry plane of the sharp-edged configuration

5 SUMMARY

Detailed LDA-measurements and flow simulations have been carried out on a sharp-edged and round-edged T-piece configuration. Based on a previous publication the SST k-ω turbulence model was chosen for the simulations. It has been found that the best agreement with the data is obtained if the computational mesh is fine in the branch pipe but coarse in the main pipe. There is no conclusive explanation for this phenomenon. Generally, the simulations reproduced the measurements well but the agreement was better in the case of sharp-edged tee. The same statement can be made for the loss coefficients although the authors think that the uncertainty in the round edged case is also larger in the experiments not only in the computations. The intuitively expected influence of rounding the edge has been confirmed both by the simulations and the experiments: the branch pipe loss coefficient significantly decreased. This means that the overall energy loss also decreased since the overall energy loss is dominated by the branch pipe energy loss.

It has been found that for the sharp-edged configuration a "fixed velocity" line exists. No similar phenomenon was found in the case of the round-edged configuration.

The work can be continued in the direction of examining different cross-section ratios and different angles between main pipe and branch pipe as well as changing systematically .the radius of curvature.

ACKNOWLEDGEMENTS

The cooperation between the partners has been supported by TéT (Nr. P-25/03) on the Hungarian side and by projects GRICES 4.1.1 OMFB and FCT PBIC/C/CEG/2440/95 and POCI/EQU/56243/2004 on the Portuguese side. The help of Messrs. Katsambas and Ugron with the simulations is gratefully acknowledged.

REFERENCES

[1, 2] Vogel, G., 1926 and 1928. "Investigation of the loss in right-angled pipe branches", Mitt. Hydraulischen Instituts der Tech. Hoschul. München, Nr. 1, 75-90 (1926), n. 2, 61-64 (1928) (Translation by Voetsch, C. Technical Memorandum n. 299, US Bureau of Reclamation, 1932)

[3] Gardel, A., 1957. "Les pertes de charge dansles écoulements au travers de branchements en Té", Bulletin Technique de la Suisse Romande, Nr. 9 & 10

[4] Maia, R. J., 1992, "Numerical and experimental investigations of the effect of local losses in piping systems. Methods and Techniques for its systematic investigation. The specific case of the flow in a 90° Tee junction" PhD thesis, University of Porto, Portugal (in Portuguese)

[5] Miller D. S., 1978, „Internal flow systems", BHRA Fluid Engineering,

[6] Sierra-Espinosa, F. Z., Bates, C. J., O'Doherty, J., 2000, „Turbulent flow in a 90º pipe junction. Part 1.: Decay of fluctuation upstream of the flow bifurcation", *Computers and Fluids* Vol. 29, pp. 197-213

[7] Sierra-Espinosa, F. Z., Bates, C. J., O'Doherty, J., 2000, „Turbulent flow in a 90º pipe junction. Part 2.: Reverse flow at the branch exit", *Computers and Fluids* Vol. 29, pp. 215-233

[8] Paál, G., Maia, R. and Pinho, F. T., 2003. Numerical predictions of turbulent flow in a 90 tee junction. *Proceedings of 12th International Conference on Modelling Fluid Flow* , Budapest, Hungary, 3rd to 6th September, paper IF0-31, pp. 573-580

[9] Menter, F., 1994. "Two equation eddy-viscosity turbulence models for engineering", *AIAA J*, 32, pp. 1598-1605.

[10] Costa, N. P. Maia, R., Pinho, F. T., & Proença, M. F. 2006 „Edge effects on the flow characteristics in a 90° T-Junction", Submitted to *ASME Journal of Fluids Engineering*.